REPORT DOCUMENTATION PAGE

Form Approved
OMB No. 0704-0188

1. REPORT DATE *(DD-MM-YYYY)*	2.REPORT TYPE	3. DATES COVERED *(From - To)*
02-26-09	Journal Article	17 Jul 08 – 07 Aug 08

4. TITLE AND SUBTITLE

Plasmon mediated, InGaAs/InP, tunable far-IR detector

5a. CONTRACT NUMBER
In-House

5b. GRANT NUMBER

5c. PROGRAM ELEMENT NUMBER
61102F

6. AUTHOR(S)

Walter Buchwald, *Robert E. Peale, Himanshu Saxena, **Brian Krejca, Mark Roland

5d. PROJECT NUMBER
2305

5e. TASK NUMBER
HC

5f. WORK UNIT NUMBER
01

7. PERFORMING ORGANIZATION NAME(S) AND ADDRESS(ES)

AFRL/RYHC, 80 Scott Drive, Hanscom AFB, MA 01731; *University of Central Florida, Department of Physics, 4000 Central Florida Blvd. Orlando, FL 32816; **Solid State Scientific Corp., Nashua, NH

8. PERFORMING ORGANIZATION REPORT

9. SPONSORING / MONITORING AGENCY NAME(S) AND ADDRESS(ES)

Electromagnetics Technology Division Source Code: 437890
Sensors Directorate
Air Force Research Laboratory/RYHC
80 Scott Drive
Hanscom AFB MA 01731-2909

10. SPONSOR/MONITOR'S ACRONYM(S)
AFRL-RY-HS

11. SPONSOR/MONITOR'S REPORT NUMBER(S)
AFRL-RY-HS-TP-2009-0004

12. DISTRIBUTION / AVAILABILITY STATEMENT
Approved for public release; distribution unlimited.

13. SUPPLEMENTARY NOTES
The U.S. Government is joint author of this work and has the right to use, modify, reproduce, release, perform, display, or disclose the work. Published in Proc. of SPIE, Vol. 7082 (2008). Cleared for Public Release by ESC-08-0984.

14. ABSTRACT

Plasmon resonances in the two dimensional electron gas (2-deg) of a high electron mobility transistor (HEMT) can affect transport properties. The resonance frequency depends on the gate-tuned sheet charge density of the 2deg and on the characteristic length of the gate metallization by which free space THz radiation couples to the plasmon. Thus, this type of device can be used as a tunable detector. This work presents an experimental investigation of such a device fabricated from the InGaAs/InP material system. E-beam lithography was used to fabricate a gate in the form of a grating with submicron period. Sensitivity of the conductance to incident THz fields is reported. Direct absorption of THz, temperature effects, and the effects of source to drain current on system performance are also investigated. It is expected that this class of device will find use in space-borne remote sensing applications.

15. SUBJECT TERMS

Plasmons, 2-deg, HEMT, active plasmonics

16. SECURITY CLASSIFICATION OF:			17.LIMITATION OF ABSTRACT	18.NUMBER OF PAGES	19a. NAME OF RESPONSIBLE PERSON
a. REPORT	b. ABSTRACT	c.THIS PAGE			Walter Buchwald
Unclassified	Unclassified	Unclassified	SAR	8	19b. TELEPHONE NUMBER *(include area code)* n/a

Standard Form 298 (Rev. 8-98)
Prescribed by ANSI Std. Z39.18

Plasmon mediated, InGaAs/InP, tunable far-IR detector

Walter R. Buchwald [a], Himanshu Saxena [b], Brian Krejca[c], Mark Roland[c] and Robert E. Peale [b]

[a] Air Force Research Laboratory, Sensors Directorate, Hanscom AFB MA 01731
[b] University of Central Florida, Physics Department, Orlando FL 32816
[c] Solid State Scientific Corporation, Nashua NH, 03049

ABSTRACT

Plasmon resonances in the two dimensional electron gas (2-deg) of a high electron mobility transistor (HEMT) can affect transport properties. The resonance frequency depends on the gate-tuned sheet charge density of the 2deg and on the characteristic length of the gate metallization by which free space THz radiation couples to the plasmon. Thus, this type of device can be used as a tunable detector. This work presents an experimental investigation of such a device fabricated from the InGaAs/InP material system. E-beam lithography was used to fabricate a gate in the form of a grating with sub-micron period. Sensitivity of the conductance to incident THz fields is reported. Direct absorption of THz, temperature effects, and the effects of source to drain current on system performance are also investigated. It is expected that this class of device will find use in space-borne remote sensing applications.

Keywords: Plasmons, 2-deg, HEMT, active plasmonics

1. INTRODUCTION

A surface plasmon is a predominantly transverse oscillation of charge at the interface between a dielectric and a negative permittivity material [1]. Although metals are traditionally used to support these oscillations, other materials, such as silicides, and two dimensional electron gasses (2degs) [2, 3], have also been used. In the case of 2degs, controlling the two dimensional sheet charge concentration via an external bias in devices such as high electron mobility transistors (HEMTs) and Si MOSFETs, leads directly to external control of the allowed plasmon resonance. In all cases, plasmon excitation via optical means is hampered by the momentum mismatch between the excitation field and the subsequent plasmon oscillation. The plasmon momentum always exceeds the photon momentum. Various methods have been developed to address this issue with one common approach being to use a grating which supplies momentum in integral multiples of $2\pi/p$ where p is the grating period. This need for a grating, and the desire to externally control the allowed resonance, leads to a new class of active plasmonic detector based on either a traditional Si MOSFET or HEMT structure [3,4]. In these devices, the gate is fabricated into a grating and serves the dual purpose of supplying the required momentum as well as controlling the sheet charge concentration. Such structures in the AlGaAs materials system have been shown to exhibit enhanced source to drain conductivity when the sheet charge, grating period and excitation wavelength are such that a plasmon resonance occurs, which therefore provide a means for the tunable detection of radiation.

This work reports on a plasmon based tunable far-IR detector fabricated from the InGaAs/InP material system. As will be explained more fully later in this work, this material system was chosen due its high sheet charge density and low effective mass. Along with a grating period of 0.5 μm, fabricated using standard e-beam lithography techniques, this structure is predicted to operate at wavelengths shorter than those previously obtainable [3,4]. Because of its unique long wavelength, frequency agile properties, this type of detector is expected to find use as a "spectrometer-on-a-chip" in chem/bio detection/identification and space situational awareness applications.

2. DEVICE DESIGN AND FABRICATION

Plasmon generation in a 2deg is governed by the following equation [3],

Infrared Spaceborne Remote Sensing and Instrumentation XVI, edited by Marija Strojnik,
Proc. of SPIE Vol. 7082, 70820B, (2008) · 0277-786X/08/$18 · doi: 10.1117/12.793804

$$\omega_p = \sqrt{\left(\frac{n_x q^2}{m^* m}\right)\left(\frac{g_m}{e_o\left(e_b + \left(e_t Coth\left(g_m d\right)\right)\right)}\right)} \quad (1)$$

where ω_p is the plasmon frequency, n_x is the 2deg sheet charge density, m^* is the electron effective mass, m is the electron rest mass, q is the elementary charge, d is the distance from the gate to the 2deg, e_o is the permittivity of free space, e_t is the relative permittivity of the material above the 2deg, e_b is the relative permittivity below the 2deg and g_m is the grating momentum, given by $(z2\pi/p)$ where z is an integer and p is the grating period as described earlier. From this equation it is seen, that in order to obtain the highest plasmon frequencies, short grating periods, high sheet charge density and a small effective mass are desirable.

Although suitable for calculating the plasmon resonant frequency as a function of material properties, equation (1) gives no information concerning temperature effects and/or resonant line shape. In order to obtain this information the more detailed theory of Ref. [5] is used. This theory, described in relation to this device in more detail in a previous work [6], treats the grating as a non-uniform conductor which is polarized by the external optical excitation. The grating polarization in-turn modifies the sheet charge conductivity via fringing fields which is the cause of the plasmon excitation in the 2deg . Figure 1 shows the previously published calculation of temperature effects on the line shape at the resonance condition for the device of this work . As can be seen, a sharper resonance is observed as the temperature is lowered, and although resonance absorption is seen as high as 100°K the magnitude of the resonance is dramatically reduced.

The MBE grown epitaxial layer structure for the device of this work is shown in Figure 2a along with the layout of a single device in Figure 2b. The layout is that of a typical HEMT with a few notable exceptions. In order to maximize the detection of any plasmon resonance, at the expense of device switching speed, the gate length and width are 195 μm and 250 μm respectively. Also, the entire 3.5mm^2 die is designed such that any incident radiation can only pass through the gate area. An inter-level dielectric of B-staged Bisbenzocycolobutane-based polymer (BCB) was used throughout the fabrication process so that all metal layers could overlap each other in order to minimize light transmission and still maintain electrical isolation. With the addition of a metal layer around the entire device, the large area gate contact acts as an aperture to a detector that is placed behind the device during optical testing. In this way, changes in device transconductance can be directly correlated with reduced transmission through the device which occur at resonance. Fabrication was undertaken using standard optical contact lithography and a combination of wet chemical etching for the semiconductor and dry etching for the BCB dielectric. No BCB was left over the gate opening in order to maximize optical throughput. After removal of the InGaAs cap in the gate region, the gate/grating was formed in two steps. A thin (75Å) of Ti was first evaporated over the entire patterned gate area. This thickness was chosen such that incident radiation would not be substantially blocked and it was made continuous in order to achieve the most uniform gate control of the 2deg sheet charge. The gate/grating was then fabricated using e-beam lithography. After spin coating with positive tone PMMA, 30keV electrons were used to pattern the 0.25μm grating stripes with a period of 0.5μm. A metal stack of 150Å/1000Å Ti/Au was then evaporated

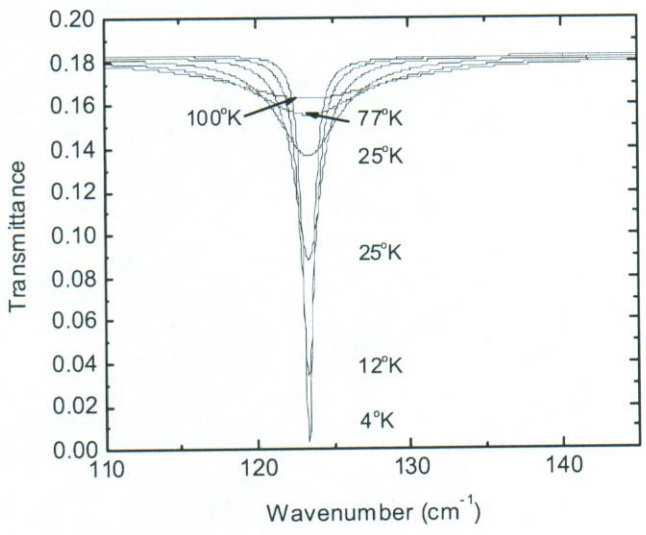

Figure 1: Simulation of reduction in transmission through the device of this work at the resonant condition as a function of temperature. Although device operation is predicted at a temperature as high as 100°K, lower temperature operation gives better performance.

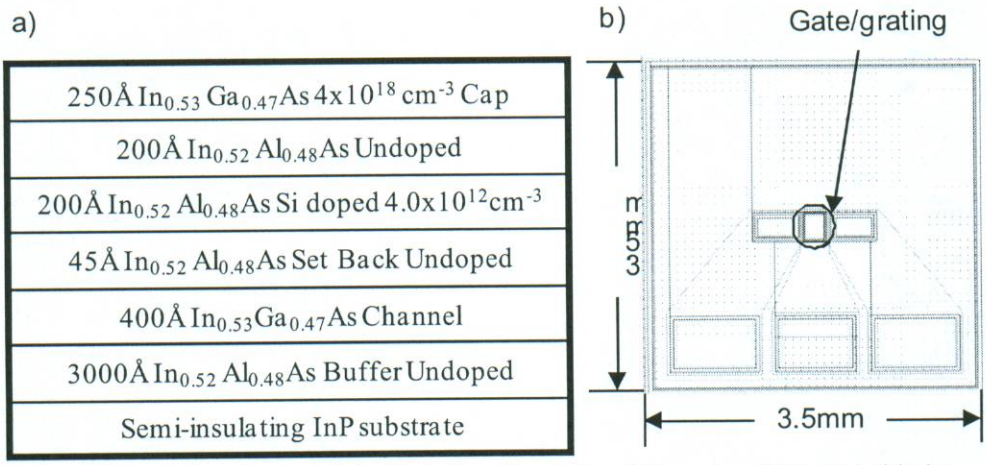

Figure 2 (a) MBE grown epilayers used for fabrication of the device of this work and (b) layout of device

and lifted completing the fabrication of the gate/grating. Figure 3 shows a SEM micrograph of the final device along with a higher magnification of the gate/grating. As seen, there appears to be slight noise problem associated with the sub-micron e-beam patterning. It is not believed that this will substantially affect the performance of the device.

To facilitate both electrical and optical measurement, a TO39 header, with a small hole drilled in the center was obtained as shown in Figure 4a. Epoxy was used to attach the device to the header with the gate/grating aperture positioned directly above the hole. Wire bonds were then used to connect the device to the header leads as shown in Figure 4b. This mounting approach was chosen so that both electrical and optical measurements could be simultaneously performed on the sample as described above.

3 DEVICE CHARACTERIZATION

Typical IV curves showing proper source/drain current saturation as well a transfer curves indicating proper gate control are shown in Figure 5a and 5b as a function of temperature. From the curves of Figure 5a an device saturation current can be obtained and in-turn, an estimate made of the actual sheet charge concentration using the following equation for saturation current [7]

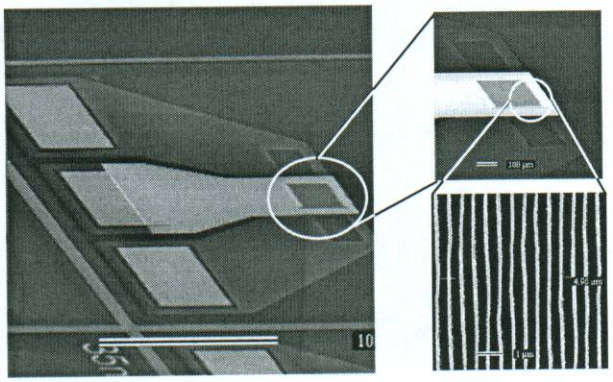

Figure 2: SEM micrograph of device used for this work

$$I_{SDSat} = qn_x \mu F_s W\left(\sqrt{(1+a^2)} - a\right) \tag{2}$$

where all values as previously defined along with F_s as the maximum electric field in the channel at the saturation velocity v_s or

$$F_s = \frac{v_s}{\mu} \tag{3}$$

With a given by

$$a = \frac{ee_o F_s L}{qn_x d} \tag{4}$$

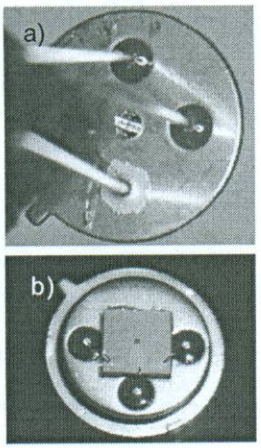

Figure 3: (a) optical port on TO-5 header and (b) mounted device.

In this equation the gate voltage dependent n_x is related to the doping in the device (n_d) through the equation

$$n_x = \frac{ee_o(V_g - V_t)}{qd} \tag{5}$$

V_t is the threshold voltage of the Schottky gate contact and is given by

$$V_t = \phi_b - E_c - \frac{qn_d d}{ee_o} \tag{6}$$

With ϕ_b the gate Schottky contact barrier height and E_c is the conduction band offset between the InGaAs and the InAlAs layers. This value, for mole fractions less than 0.54, is taken to be [8]

$$E_c = 0.384 + 0.254x \tag{7}$$

By measuring the saturation current as a function of both gate bias and temperature, the above equations can be used to extract the temperature dependant mobility, μ, and the effective device doping, n_d. These values can then be used to determine the 2deg sheet charge concentration, n_x, needed to extract the plasmon resonance condition from equation (1) above. For this work the following values for all previously defined terms used in simulations and curve fitting are as follows: W=195μm, L=250μm, d=445Å, x=0.532, ϕ_b=0.7eV, v_s = 1.6x10^5(m/s), e_t=11.7, e_b=12.0, m^*=0.041.

Figure 6 shows the gate bias saturation current data reduction described above. And the inset shows the extracted values for μ, n_d, and n_x as functions of temperature. Room temperature Hall measurements were also performed on these samples. In this case, the InGaAs cap was first removed by chemical etching and the material cleaved into a square. Ohmic contacts were added to the four corners of the square with In solder in order to facilitate the Hall measurements. The results indicate a sheet charge concentration of 1.172x10^{12} cm^{-2} and a mobility of 11331 cm^2/Vs. This is within a factor of 2 that was obtained from the I_{sat} curve fitting method. It is not immediately understood what causes this discrepancy. In both cases, the InGaAs cap is removed, however, in the Hall measurement case it is removed from the

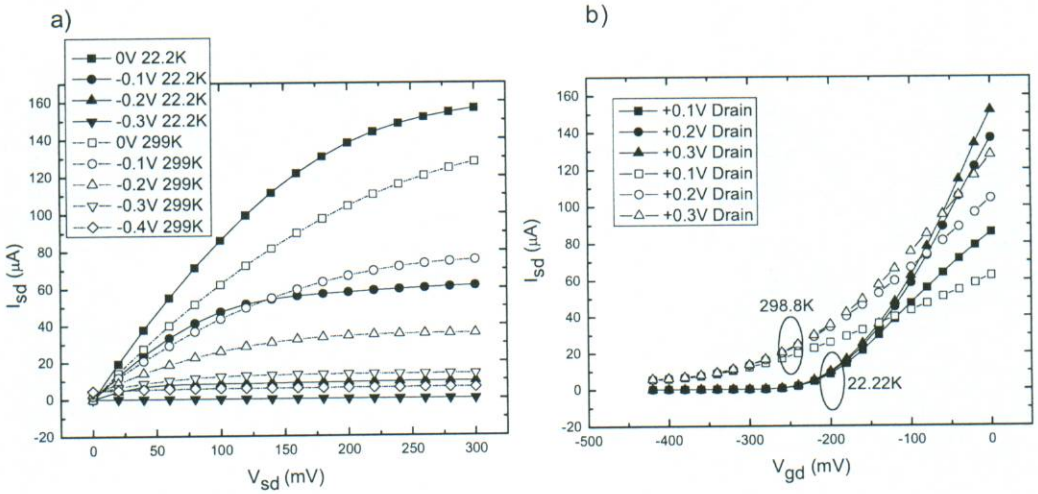

Figure 4: (a) Source/Drain current as a function of Source/Drain bias at various gate voltages and (b) Source/Drain current as a function of gate bias at various Drain biases for the device of this work.

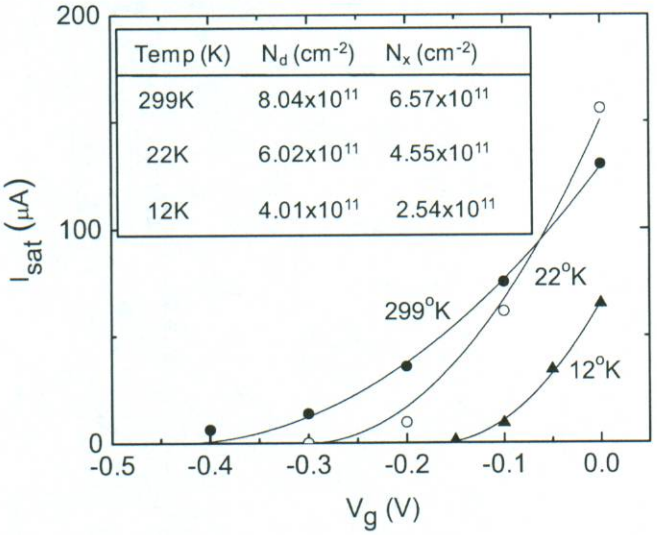

Figure 5: Curve fits of saturation current as a function of gate bias at various temperatures used to determine mobility and 2deg sheet charge concentration

entire sample and in the I_{sat} measurement case it is only removed in the gate area. It is suggested that in the I_{sat} measurement case, the addition of the gate contact could cause slight increase in surface depletion which might alter the 2deg sheet charge concentration. In any case, in the subsequent portions of this work, the values of sheet charge concentration obtained by the I_{sat} measurement technique will be used.

All of the information is now available to determine over what range of excitation energies plasmon resonance would expect to be seen. Using a grating period of 0.5μm, Figure 7 shows the 2deg sheet charge density as a function of gate bias. From this plot, the 2deg sheet charge density values of $5.8x10^{15}$ (m^{-2}) and $1x10^{14}$ (m^{-2}), along with Equation (1), can be used to determine the maximum and minimum excitation wavelengths of 1130μm (270 GHz) and 148.5μm (2.12 THz). In this plot, in order to extend the range of accessible wavelengths, the gate voltage was swept from -0.2V to +0.3V. The positive value of 0.3 V is justified as still being able to control the 2deg sheet charge concentration while still not allowing the Schottky gate diode contact to not turn fully on, as 0.3 V is less than half the turn on voltage of 0.7 V which is typical for III-V Schottky contacts.

4 OPTICAL CHARACTERIZATION

Three approaches to optical characterization have commenced as of this writing. In the first, the device in its TO39 can is mounted at the end of a copper cold finger in a Janis SHI-4 closed cycle refrigerator. A Si diode thermometer is mounted next to the device on the same cold head and shows that a temperature of 12°K is reached. Polarized radiation from a backward wave oscillator (BWO) tunable from 75 to 110 GHz is incident on the device through a polyethylene window. The BWO is amplitude modulated using an external TTL square wave. The BWO output is monitored with a crystal detector mounted on a directional coupler and observed on an oscilloscope. The device drain is connected to ground through a 50 ohm resistor. The source voltage is fixed, and the gate voltage is stepped in small increments from 0 to -0.3 V while the BWO is swept repeatedly through its frequency range. The drain current is measured as the voltage drop across the 50 ohm resistor, and is synchronously lock-in amplified. The output of the lock-in is recorded on a strip chart. If the BWO sweeps through the resonance frequency of the device, we look for any repeatable

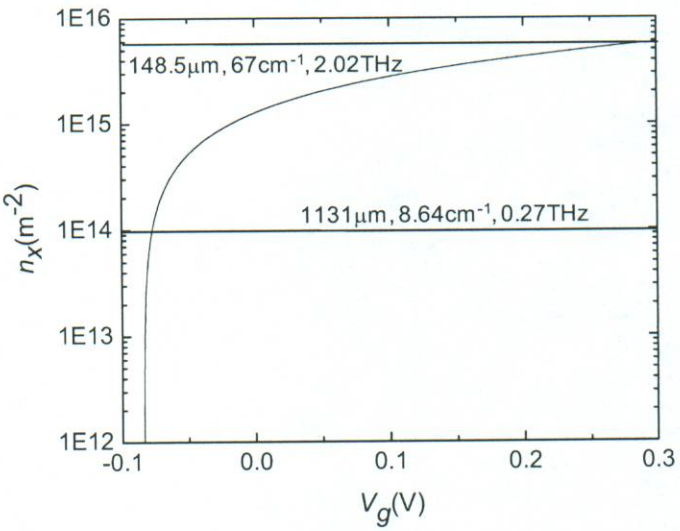

Figure 6: Calculated 2deg sheet charge density as a function of gate bias for the device of this work. Wavelength range for plasmon excitation is also shown.

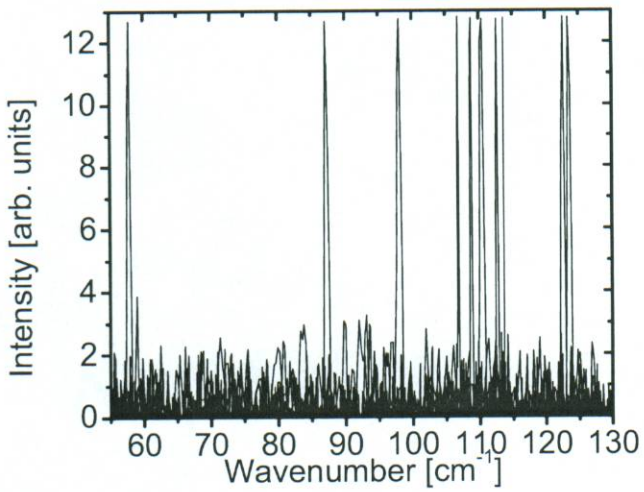

Figure 7: Superposition of p-Ge laser narrow-line emission spectra. Except for the line near 58 cm^{-1}, all narrow-band emission lines are achieved using intracavity etalons. The line at 58 cm^{-1} in the so-called "low-field" regime of laser operation is naturally narrow due to resonance with gallium impurity levels

change in the drain current. As of this writing, only preliminary observations have been undertaken and no mm-wave effect has yet been recorded. A number of possible reasons are being explored. One is that the grating period on the first device prepared and tested is not optimized for microwave frequencies, such that the slope of the curve of the resonance frequency with gate voltage is exceptionally steep. This means that the resonance might easily be missed. We do not yet have an accurate measure of the microwave power actually incident on the sample, and the polarization of the microwaves has not yet been taken into account. Plans are underway to modulate the gate voltage at fixed BWO frequency in hopes that this will produce a sharper and more dramatic effect.

The second approach to use a p-type Ge laser [9], which, in principle, is tunable from 1.5 to 4.2 THz. The laser operates in a liquid helium bath at 4 K, produces a ~1 μs long pulse at a repetition rate of 1-4 Hz. Fig. 8 shows some laser emission lines, measured by high resolution FTIR, that have been produced using intracavity etalons as wavelength selectors. In first experiments, the laser was operated without a selector, so that the emission spectrum is likely an irregular band spanning ~20 cm^{-1} somewhere in the range 70-130 cm^{-1} with a peak output power on the order of 1 W [9]. A small hole is drilled in the back of the TO39 can to allow the transmission of the THz radiation to a 4K Ge:Ga photodetector that is carefully shielded from stray radiation. A 100 micron aperture is placed before the detector to avoid saturation and to keep the detector response in the linear regime. Then with source and drain grounded, the gate voltage is stepped in steps of 0.5 mV over the range -0.3 to 0.3 V, while monitoring the detector signal on an oscilloscope. A decrease in the signal strength corresponding to absorption in the device under the gate is sought. Next, the voltage drop is monitored at the 50 ohm load attached to the drain. Changes in drain current synchronous with the laser pulse are sought. In first experiments, neither transmission or conductance changes have been observed. Small changes in drain current were masked by large electromagnetic interference (EMI) due to the pulsing of the laser (dI/dt~100 A/100 ns) in close proximity to device leads. Additionally, based on fitting of low temperature IV curves, we believe the resonance frequency of the device may be below the emission frequency of the laser due to insufficiently high sheet charge density. Under special conditions, the laser can be made to emit at 58 cm^{-1} in a single emission line without need of a wavelength selector in the so-called "low-field" regime of laser operation [10]. This requires exceptional operating conditions for the laser that we are now attempting to achieve. Whether the sheet charge density is sufficient at 4°K for the given grating structure to produce a resonance at 58 cm^{-1} is still a question under investigation.

The third method of optical characterization is the first to give an indication of the desired plasmon absorption. In this experiment, the device is mounted at the end of the light baffle of a 4 K silicon bolometer (IR labs). Since the device is not in direct contact with the 4 K cold plate, its temperature is somewhat elevated. The opening to the bolometer is carefully screened so that all radiation reaching the bolometer must have passed through the gate region of the device. The sample is mounted in this unconventional way to achieve close coupling of the bolometer to the sample, since diffraction at the small gate aperture leads to rapid divergence of the beam. The bolometer then records the modulated light from a Fourier spectrometer in the 10-50 cm^{-1} range using 50 micron mylar pellical beamsplitter and Hg arc lamp. A wire-grid on polyethylene polarizer is used, and a strong polarization effect is observed. When the electric field vector is parallel to the direction of the grating lines, no transmitted signal could be detected. When the electric field vector is rotated to be perpendicular of the grating lines, sufficient signal is transmitted to record a power spectrum. Figure 9 presents the transmitted intensity for different applied gate voltages with both source and drain grounded. There are strong rapid oscillations due to Fabry-Perot resonance in the plane parallel semiconductor device. At certain wavenumber positions indicated by arrows, we observe a near cancellation of the oscillations, indicating that the sample is absorbing at these wavenumbers. For zero gate bias, these disturbances are located at 24 and 48 cm^{-1}. The lower

wavenumber disturbance is close to the estimated 30 cm^{-1} fundamental resonance frequency estimated from the sheet charge density, and we attribute this feature to the fundamental plasmon resonance. The disturbance at 48 cm^{-1} is the harmonic. As negative gate voltage is applied, the two features shift to lower wavenumbers as expected. At a gate bias of -0.1 V, the resonances appear at 18 and 36 cm^{-1}. At a bias of -0.2 V, they have shifted down to 16 and 32 cm^{-1}, and a new harmonic has emerged at 48 cm^{-1}. The presence of harmonics and the shift with bias agree with theoretical expectations for the plasmon resonances and confirm their observation in our device.

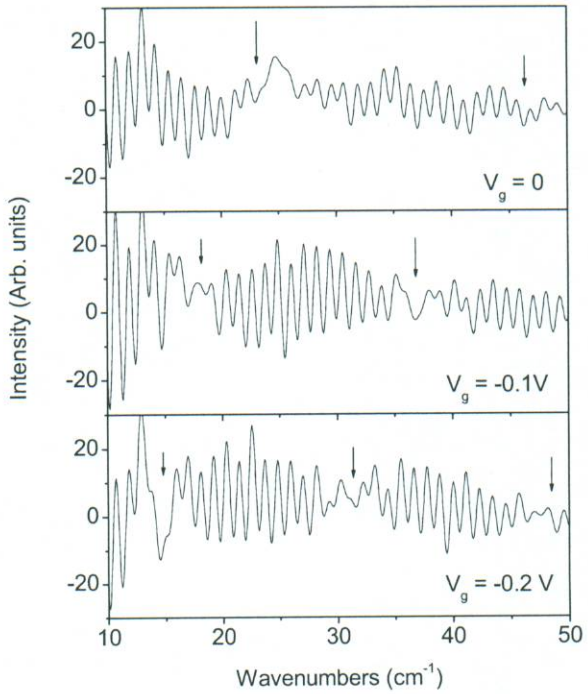

5 CONCLUSION

A plasmon mediated, 2deg based, resonant detector has been designed, fabricated and characterized from the InGaAs/InP material system. Although electrical characterization reveals acceptable 2deg sheet charge control via the gate bias, the 2deg sheet charge is less than anticipated for the epi-layer structure used. This reduced sheet charge caused the predicted plasmon resonance to fall in a region difficult to explore with either the BWO or p-Ge laser, but accessible to the Fourier spectrometer. Experiments with the latter instrument reveal clear evidence of the plasmon resonances. Work is underway to redesign the metallization to allow larger gate areas and throughput, to make gate gratings that give plasmon resonances in the mm-wave region, and to consider higher intensity tunable sources (e.g. the UCSB FEL) for characterization.

6. ACKNOWLEDGEMENTS

The authors of this work would like to acknowledge funding for this work from the Air Force Office of Scientific Research Tasks 06SN05COR and 92SN06COR. REP and HS acknowledge AFRL contract FA871807C0036.

REFERENCES

[1] Rather, H., "Surface Plasma Oscillations and Their Applications" , [Physics of Thin Films], Academic, New York, 145 (1977)

[2] Soref, R., Peale, R. E. and Buchwald, W. "Longwave plasmonics on doped silicon and silicides", Optics Express, **16**, 6507 (2008)

[3] Allen, S.J., Tsui, D.C., Logan, R. A., "Observation of the two-dimensional Plasmon in silicon inversion layers," Phys. Rev. Lett. **38**, 980 (1977).

[4] Peralta,X.G., Allen, S.J., Wanke, M.C., Harff, N.E., Simmons, J.A., Lilly, M.P., Reno, J.L., Burke ,P.J. and Eisenstein, J.P., "Terahertz photoconductivity and Plasmon modes in double-quantum-well field-effect transistors," Appl. Phys. Lett, **86**, 1627 (2002).

[5] Zheng,L., W. Schaich ,L., and MacDonald , A. H., "Theory of two-dimensional grating couplers", Phys. Rev. B **41**, 8493 (1990).

[6] Buchwald, W. R., Saxana, H., Peale, R.E., "Tunable Far-IR Detectors/Filters Based on Plasmons in Two Dimensional Electron Gases in InGaAs/InP Heterostructures" SPIE-Optics and Photonics, Infrared Spaceborne Remote Sensing and Instrumentation XV (OP401), San Diego CA, August (2007)

[7] Grinberg , A.A., Shur , M., "A new analytical modal for heterostructure field effect transistors", J. Appl. Phys., **65,** 2116 (2008)

[8] Huang, J.-H., Chang, T. Y., and Lalevic , B., "Measurement of the conduction-band discontinuity in pseudomorphic $In_xGa_{1-x}As/In_{0.52}Al_{0.48}As$ heterostructures," Appl. Phys. Lett. **60**, 733 (1992).

[9] Muravjov, V., Saxena, H., Peale, R.E., Fredricksen, C. J., Edwards, O., and Shastin, V. N., "Injection-seeded internal-reflection-mode p-Ge laser exceeds 10 W peak terahertz power," J. Appl. Phys. 103, 083112 (2008).

[10] Park, K., Peale, R. Weidner, E., H., and Kim , J. J. ,"Submillimeter p-Ge laser using a Voigt-configured permanent magnet,",IEEE J. Quantum Electronics 32, 1203-1210 (1996).